

Efficient calculation of chiral three-nucleon forces up to N³LO for ab initio studies

K. Hebeler,^{1,2,*} H. Krebs,^{3,†} E. Epelbaum,^{3,‡} J. Golak,^{4,§} and R. Skibiński^{4,¶}

¹*Technische Universität Darmstadt, 64289 Darmstadt, Germany*

²*ExtreMe Matter Institute EMMI, GSI Helmholtzzentrum für Schwerionenforschung GmbH, 64291 Darmstadt, Germany*

³*Institut für Theoretische Physik II, Ruhr-Universität Bochum, D-44780 Bochum, Germany*

⁴*M. Smoluchowski Institute of Physics, Jagiellonian University, PL-30348 Krakow, Poland*

We present a novel framework to decompose three-nucleon forces in a momentum space partial-wave basis. The new approach is computationally much more efficient than previous methods and opens the way to ab initio studies of few-nucleon scattering processes, nuclei and nuclear matter based on higher-order chiral 3N forces. We use the new framework to calculate matrix elements of chiral three-nucleon forces at N²LO and N³LO in large basis spaces and carry out benchmark calculations for neutron matter and symmetric nuclear matter. We also study the size of the individual three-nucleon force contributions for ³H. For nonlocal regulators, we find that the sub-leading terms, which have been neglected in most calculations so far, provide important contributions. All matrix elements are calculated and stored in a user-friendly way, such that values of low-energy constants as well as the form of regulator functions can be chosen freely.

PACS numbers: 21.30.-x, 21.45.Ff, 13.75.Cs

I. INTRODUCTION

The importance of chiral three-nucleon (3N) forces has been demonstrated in numerous microscopic calculations of few-body scattering processes, nuclei and nuclear matter, see [1, 2] for recent review articles. Contributions to 3N forces (3NFs) start to appear at next-to-next-to-leading-order (N²LO) in the chiral expansion within Weinberg's power counting framework [3–6], whereas the subleading chiral 3NFs at next-to-next-to-next-to-leading-order (N³LO) have the particular feature that they do not include any new low-energy constants [7–9]. So far, all microscopic calculations for finite nuclei of mass $A > 3$ based on chiral EFT interactions were limited to 3NFs at leading order (N²LO), whereas NN forces are commonly included up to N³LO, see [10] for a fifth order analysis of NN scattering. For NN forces, it is known that N³LO contributions are important for a high-precision fit of scattering phase shifts and mixing angles up to laboratory energies of $E \sim 200$ MeV [5, 11–15]. It is clearly desirable to extend these studies and perform *complete* N³LO calculations, which would require the inclusion of subleading N³LO 3N contributions, see Refs. [16–18] for first calculations along this line. In fact, such studies are a central goal of the recently formed Low Energy Nuclear Physics International Collaboration (LENPIC) [19].

In particular, one may expect that the unresolved discrepancies for spin-dependent nucleon-deuteron (Nd) scattering observables between calculations based on high-precision phenomenological NN and 3NF models

and experimental data at intermediate and higher energies cannot be probed at the N²LO level of accuracy. Furthermore, recent advances in nuclear structure theory make it possible to extend the range of ab initio calculations to mass numbers of $A = 132$ [20]. The inclusion of 3NF contributions beyond the leading ones in few- and many-body calculations is the key for increasing the accuracy of predictions for nuclear observables and for systematic investigations of the role of chiral symmetry in nuclei and nuclear matter. We also note that corrections to the 3NF beyond N²LO (see Fig. 1) contain such contributions, which have already been found earlier in phenomenological interaction models to be important for the accurate description of properties of light nuclei [21].

Numerous N²LO calculations of Nd scattering at low energy have revealed, generally, a good agreement between theory and experimental data, see [5, 22] and references therein. On the other hand, the well-known discrepancies such as, e.g., the A_y puzzle and the cross section in the symmetric space star configuration of the deuteron break up process could not be resolved at this chiral order [1]. Promising results based on chiral 3NFs at N²LO were reported by various groups in nuclear structure calculations showing, in particular, sensitivity to the individual 3NF contributions, see Refs. [2, 23] for review articles. Also recent lattice simulations and no-core shell model calculations of light nuclei within chiral effective field theory demonstrate clearly the important role of the N²LO 3NFs (see e.g., Refs. [24–28]). Furthermore, for neutron-rich systems, contributions from 3NFs have been shown to be of critical importance for the shell structure and stability close to the neutron drip line (see, e.g., [29–34]), while for nuclear matter, saturation was demonstrated to be driven by 3NFs [35, 36].

While the formal expressions for the individual contributions of all the topologies shown in Fig. 1 have already been worked out [8, 9], their decomposition in a suitable

* E-mail: kaihebeler@physik.tu-darmstadt.de

† E-mail: Hermann.Krebs@tp2.ruhr-uni-bochum.de

‡ E-mail: Evgeny.Epelbaum@ruhr-uni-bochum.de

§ E-mail: ufgolak@cyf-kr.edu.pl

¶ E-mail: roman.skibinski@uj.edu.pl

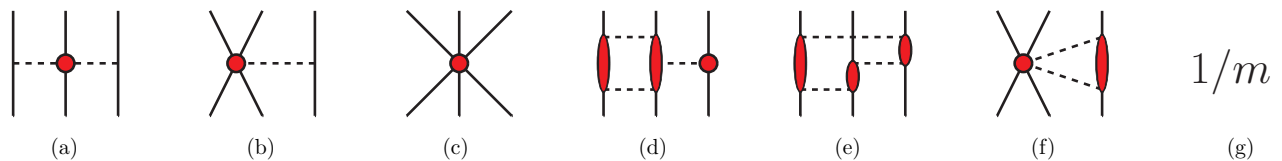


FIG. 1. (color online) Different topologies that contribute to the chiral 3NF up to $N^3\text{LO}$ (and $N^4\text{LO}$). Nucleons and pions are represented by solid and dashed lines, respectively. The shaded vertices denote the amplitudes of the corresponding interaction. Specifically, the individual diagrams are: (a) 2π exchange, (b) 1π -contact, (c) pure contact, (d) 2π - 1π exchange, (e) ring contributions, (f) 2π -contact and (g) relativistic corrections. See main text for details.

form for few- and many-body frameworks represents a highly nontrivial task [37–39]. Due to the huge amount of computational resources needed for this decomposition, matrix elements have been so far available only in a limited model space [16]. As a consequence, consistent $N^3\text{LO}$ three-body scattering calculations were limited to low energies and no studies of heavier nuclei were possible. In this paper we present a novel framework that allows one to decompose 3N interactions in a plane-wave partial wave basis in a computationally much more efficient way than the framework of Refs. [38, 39]. This new method makes explicit use of the fact that all (unregularized) contributions to chiral 3NFs are either local, i.e. they depend only on momentum transfers, or they contain only polynomial non-local terms.

In Section II we derive the new framework for decomposing local 3NFs efficiently in a momentum-space partial wave basis. In Section III we apply the calculated matrix elements of chiral 3NFs up to $N^3\text{LO}$ to nuclear matter and ^3H , discuss the partial wave convergence and investigate the importance of the individual topologies at different orders in the chiral expansion. In Section IV we summarize and give an outlook of future applications.

II. PARTIAL WAVE DECOMPOSITION OF LOCAL THREE-NUCLEON FORCES

A general translationally invariant 3NF can be expressed as a function of the Jacobi momenta $\mathbf{p} = \frac{\mathbf{k}_1 - \mathbf{k}_2}{2}$ and $\mathbf{q} = \frac{2}{3} [\mathbf{k}_3 - \frac{1}{2}(\mathbf{k}_1 + \mathbf{k}_2)]$, where \mathbf{k}_i denote the single nucleon momenta (in the following equations we will first suppress spin and isospin degrees of freedom):

$$V_{123} = V_{123}(\mathbf{p}, \mathbf{q}, \mathbf{p}', \mathbf{q}'). \quad (1)$$

Here and in the following \mathbf{p} and \mathbf{q} (\mathbf{p}' and \mathbf{q}') denote the Jacobi momenta of the initial (final) state. For local interactions, however, the momentum dependence further simplifies as such forces only depend on momentum transfers, i.e. on differences of Jacobi momenta:

$$V_{123}^{\text{loc}} = V_{123}^{\text{loc}}(\mathbf{p}' - \mathbf{p}, \mathbf{q}' - \mathbf{q}) \equiv V_{123}^{\text{loc}}(\tilde{\mathbf{p}}, \tilde{\mathbf{q}}). \quad (2)$$

Note that this statement refers to unregularized forces. Below we will apply non-local regulators to the partial-wave decomposed matrix elements. The regularization will be discussed in more detail in Section III.

Generally, the decomposition of 3NFs in plane-wave partial waves involves the evaluation of projection integrals of the form

$$F_{LL'L'}^{m_L m_L' m_L' m_L'}(p, q, p', q') = \int d\hat{\mathbf{p}}' d\hat{\mathbf{q}}' d\hat{\mathbf{p}} d\hat{\mathbf{q}} \\ \times Y_{L'm_L'}^*(\hat{\mathbf{p}}') Y_{l'm_L'}^*(\hat{\mathbf{q}}') Y_{Lm_L}(\hat{\mathbf{p}}) Y_{l m_l}(\hat{\mathbf{q}}) V_{123}^{\text{loc}}(\tilde{\mathbf{p}}, \tilde{\mathbf{q}}) \quad (3)$$

for fixed values of $p = |\mathbf{p}|$, $q = |\mathbf{q}|$, $p' = |\mathbf{p}'|$, $q' = |\mathbf{q}'|$ and the angular momentum quantum numbers. By using symmetries, it is possible to reduce the dimensionality of the angular integrals from 8 to 5. Traditional methods are based on a direct discretization and numerical evaluation of these angular integrals [38, 39]. Due to the large number of external quantum numbers and momentum mesh points such algorithms require very large computational resources for calculating all matrix elements necessary for many-body studies. As a result, the number of matrix elements of chiral $N^3\text{LO}$ interactions were so far insufficient for studies of nuclei and matter. However, it is possible to evaluate the basic function F defined in Eq. (3) in a much more efficient way by explicitly making use of the local nature of the 3NFs. Indeed, using rotation invariance of the potential V_{123}^{loc} we can write it as a function of three independent variables:

$$V_{123}^{\text{loc}}(\tilde{\mathbf{p}}, \tilde{\mathbf{q}}) = V_{123}^{\text{loc}}(\tilde{p}, \tilde{q}, \cos \theta_{\tilde{\mathbf{p}}\tilde{\mathbf{q}}}), \quad (4)$$

where

$$\cos \theta_{\tilde{\mathbf{p}}\tilde{\mathbf{q}}} = \frac{\tilde{\mathbf{p}} \cdot \tilde{\mathbf{q}}}{\tilde{p}\tilde{q}}, \quad \tilde{p} = |\tilde{\mathbf{p}}|, \quad \tilde{q} = |\tilde{\mathbf{q}}|. \quad (5)$$

This already shows that the original eight-dimensional integral contains actually only three non-trivial integrations. The other five integrations, after employing some integral transformations, which are described in the appendix, can be performed analytically. The final result

is given by

$$\begin{aligned}
& F_{LL'L'}^{m_L m_{L'} m_{L'}}(p, q, p', q') \\
&= \delta_{m_L - m_{L'}, m_{L'} - m_L} (-1)^{m_L + m_{L'}} \frac{2(2\pi)^4}{pp'qq'} \\
&\times \sum_{\bar{l}=\max(|L'-L|, |l'-l|)}^{\min(L'+L, l'+l)} \frac{C_{L'-m_{L'}, L m_L}^{\bar{l}-m_{L'}+m_L} C_{l'-m_{L'}, l m_L}^{\bar{l}-m_{L'}+m_L}}{2\bar{l}+1} \\
&\times \int_{|p'-p|}^{p'+p} d\tilde{p} \tilde{p} \int_{|q'-q|}^{q'+q} d\tilde{q} \tilde{q} \\
&\times \mathcal{Y}_{L'L}^{\bar{l}0}(\widehat{\tilde{p}\mathbf{e}_z + \mathbf{p}}, \hat{\mathbf{p}}) \Big|_{\phi_p=0, \hat{p}\cdot\mathbf{e}_z = \frac{p'^2 - p^2 - \tilde{p}^2}{2p\tilde{p}}} \\
&\times \mathcal{Y}_{l'l}^{\bar{l}0}(\widehat{\tilde{q}\mathbf{e}_z + \mathbf{q}}, \hat{\mathbf{q}}) \Big|_{\phi_q=0, \hat{q}\cdot\mathbf{e}_z = \frac{q'^2 - q^2 - \tilde{q}^2}{2q\tilde{q}}} \\
&\times \int_{-1}^1 d \cos \theta_{\tilde{p}\tilde{q}} P_{\bar{l}}(\cos \theta_{\tilde{p}\tilde{q}}) V_{123}^{\text{loc}}(\tilde{q}, \tilde{p}, \cos \theta_{\tilde{p}\tilde{q}}) \quad (6)
\end{aligned}$$

with

$$\mathcal{Y}_{l_a l_b}^{LM}(\hat{\mathbf{a}}, \hat{\mathbf{b}}) = \sum_{m_a, m_b} C_{l_a m_a l_b m_b}^{LM} Y_{l_a}^{m_a}(\hat{\mathbf{a}}) Y_{l_b}^{m_b}(\hat{\mathbf{b}}). \quad (7)$$

Realistic nuclear forces also depend on the spin and isospin quantum numbers of the nucleons. As a complete basis, we choose the standard Jj -coupled three-body plane-wave basis of the form [40]

$$|pq\alpha\rangle \equiv |pq; [(LS)J(ls)j] \mathcal{J}(Tt)\mathcal{T}\rangle, \quad (8)$$

where L , S , J and T denote the relative orbital angular momentum, spin, total angular momentum and isospin of particles 1 and 2 with relative momentum p . The quantum numbers l , $s = 1/2$, j and $t = 1/2$ label the orbital angular momentum, spin, total angular momentum and isospin of particle 3 relative to the center-of-mass of the pair with relative momentum p . The quantum numbers \mathcal{J} and \mathcal{T} define the total three-body angular momentum and isospin (for details see Ref. [40]). In Eq. (8) we have used the fact that the 3NFs do not depend on the projections $m_{\mathcal{J}}$ and $m_{\mathcal{T}}$, hence we omit these quantum numbers in the basis states here and in the following. The detailed basis sizes for the different three-body channels for our calculations of $N^3\text{LO}$ matrix elements are presented in Table I. Notice that as will be shown below, it is sufficient for our purposes to truncate the value of the total three-body angular momentum at $\mathcal{J} = 9/2$. We have also verified that further increasing the values of J_{max} leads to negligibly small effects for all performed calculations. However, for future studies of heavier nuclei we could extend the calculations to even larger \mathcal{J} and J_{max} , if necessary.

Due to the explicit momentum dependence of the spin-momentum operators, the knowledge of the function F in Eq. (3) is, in general, not sufficient and the framework needs to be extended. This can be done in a straightforward way by factorizing out the momentum dependence

TABLE I. Dimension and file size of the individual 3NF matrix element files up to $N^3\text{LO}$ for the different three-body partial waves. All matrix elements are calculated and stored in such a way that values of the low-energy couplings $c_1, c_3, c_4, c_D, c_E, C_S$ and C_T can be chosen freely for the different topologies, leading to in total 12 files for each partial wave (see main text). For all partial waves $N_p = N_q = 15$ has been used. N_α denotes the number of partial-wave channels defined in Eq. (8). All given values apply to both three-body parities.

\mathcal{J}	\mathcal{T}	J_{max}	N_α	filesize [GB]
1/2	1/2	8	66	0.8
3/2	1/2	8	126	3.0
5/2	1/2	8	178	6.0
7/2	1/2	7	190	6.8
9/2	1/2	6	178	6.0
1/2	3/2	8	34	0.2
3/2	3/2	8	65	0.8
5/2	3/2	8	92	1.6
7/2	3/2	7	91	1.6
9/2	3/2	6	94	1.7

of spin-momentum operators in the form

$$\boldsymbol{\sigma} \cdot \mathbf{x} = \sqrt{\frac{4\pi}{3}} x \sum_{\mu=-1}^1 Y_{1\mu}^*(\hat{\mathbf{x}}) \boldsymbol{\sigma} \cdot \mathbf{e}_\mu \quad (9)$$

and combining the additional spherical harmonic function with the ones in Eq. (3) by using

$$Y_{lm}(\hat{\mathbf{x}}) Y_{1\mu}(\hat{\mathbf{x}}) = \sum_{\bar{L}=|l-1|}^{l+1} \sqrt{\frac{3}{4\pi} \frac{2l+1}{2\bar{L}+1}} C_{l010}^{\bar{L}0} C_{lm1\mu}^{\bar{L}m+\mu} Y_{\bar{L}m+\mu}(\hat{\mathbf{x}}), \quad (10)$$

where \mathbf{x} represents a Jacobi momentum. This strategy makes it possible to reduce the expressions for arbitrary spin-dependent interactions to the expression for spin-independent interactions times some momentum-independent spin operators. This step has to be performed for each momentum vector in the spin-momentum operators. Obviously, the efficiency of the present algorithm decreases with each additional sum over the quantum numbers μ and \bar{L} in Eqs. (9) and (10). Note, however, that each of these sums contains only three terms at most.

In order to factorize the momentum, spin and isospin space, for practical calculations we first calculate the interaction matrix elements in a LS -coupled basis:

$$|pq\beta\rangle \equiv |pq; [(Ll)\mathcal{L}(Ss)\mathcal{S}] \mathcal{J}(Tt)\mathcal{T}\rangle, \quad (11)$$

and recouple only at the end to the Jj -coupled basis defined in Eq. (8). Each time the factorization in Eq. (9) is applied, the spin matrix element effectively becomes

dependent on the quantum number μ , i.e. generally the matrix element in spin space can be written in the form

$$\left\langle (Ss)\mathcal{S}m_S|\hat{O}_\sigma(\{\mu_i\})|(S's')\mathcal{S}'m_{S'}\right\rangle, \quad (12)$$

where the index i counts the number of momentum vectors in the spin operator. In the same way the function F in Eq. (3) becomes a function of the quantum numbers μ_i , i.e. it takes the form $F_{L\bar{L}L'L'}^{m_L m_L' m_L'' m_L'''}\{\mu_i\}$. To be explicit, if we consider, e.g., the case $\mathbf{x} = \mathbf{p}$ in Eq. (9), the function F takes the form

$$F_{L\bar{L}L'L'}^{m_L m_L' m_L'' m_L'''}(p, q, p', q') = p \sum_{\bar{L}=|L-1|}^{L+1} \sqrt{\frac{2L+1}{2\bar{L}+1}} \times \mathcal{C}_{L010}^{\bar{L}0} \mathcal{C}_{Lm_L+\mu}^{\bar{L}m_L+\mu} F_{\bar{L}L'L'}^{m_L m_L' m_L'' m_L'''}(p, q, p', q'), \quad (13)$$

where we included the factor $\sqrt{\frac{4\pi}{3}}p$ from the spin operator factorization in Eq. (9) in this function.

For an efficient calculation it is important to note that all quantities that depend on the projection quantum numbers m and μ are momentum independent. Hence, it is advantageous to factorize this dependence in the function F . Specifically, for the example shown in Eq. (13) we can write

$$F_{L\bar{L}L'L'}^{m_L m_L' m_L'' m_L'''}(p, q, p', q') \equiv \delta_{m_L - m_{L'}, m_{L''} - m_{L'''}} (-1)^{m_L + m_{L''}} \times \sum_{\bar{l}} \mathcal{C}_{L' - m_{L'}, L m_L}^{\bar{l} - m_{L'} + m_L} \mathcal{C}_{L' - m_{L''}, l m_L}^{\bar{l} - m_{L''} + m_L} \times \sum_{\bar{L}} \mathcal{C}_{L010}^{\bar{L}0} \mathcal{C}_{Lm_L+\mu}^{\bar{L}m_L+\mu} \tilde{F}_{\bar{L}L'L'}^{\bar{l}\bar{l}}(p, q, p', q'). \quad (14)$$

For general interactions, the function \tilde{F} depends on multiple quantum numbers \bar{L}_i , hence the function takes formally the form $\tilde{F}_{L\bar{L}L'L'}^{\bar{l}\bar{l}\{\bar{L}_i\}}(p, q, p', q')$. Using this decomposition we can first precalculate all sums over the projection quantum numbers m and μ_i and prestore the result in a function of the form $A_{\beta\beta'}^{\bar{l}\bar{l}\{\bar{L}_i\}}$. Then the final matrix element in LS -coupling can be calculated very efficiently via:

$$\langle pq\beta|V_{123}|p'q'\beta'\rangle = \sum_{\bar{l}} \sum_{\{\bar{L}_i\}} A_{\beta\beta'}^{\bar{l}\bar{l}\{\bar{L}_i\}} \tilde{F}_{L\bar{L}L'L'}^{\bar{l}\bar{l}\{\bar{L}_i\}}(p, q, p', q'), \quad (15)$$

where values of the quantum numbers L, L', l and l' are specified by the LS -coupling partial wave indices β and β' (see Eq. (11)).

Note that by deriving Eq. (15) the original problem of calculating numerically a 5-dimensional integral for each matrix element as in Eq. (3) has been reduced to the evaluation of a few discrete sums. The calculation and prestorage of the matrix elements of $\tilde{F}_{L\bar{L}L'L'}^{\bar{l}\bar{l}\{\bar{L}_i\}}(p, q, p', q')$ can be performed relatively efficiently since only three internal integrals have to be performed numerically. The exact speedup factor of the present method compared to the conventional approach [38, 39] depends on the number of internal sums over μ_i and \bar{L}_i , i.e. on the specific

form of the interaction. For example, the matrix elements of the chiral long-range interactions at N^2LO proportional to the couplings c_1 and c_3 can be calculated with speedup factors of greater than 1000. Practically, that means that it is now possible to calculate the matrix elements of all interaction terms listed in Table I up to N^3LO on a local computer cluster for sufficiently large basis sizes for studies of few-nucleon scattering processes, light and medium mass nuclei as well as nuclear matter. Obviously, the efficiency of the present method decreases with each additional internal sum in Eq. (9) and Eq. (10). However, for all 3NF topologies up to N^3LO except the relativistic corrections, we achieve speedup factors of typically $\gtrsim 100$.

Even though the present algorithm makes explicit use of the local nature of the chiral 3NFs, it is also possible to treat polynomial non-local terms. This is of immediate practical importance since the relativistic corrections at N^3LO have precisely this form [9]. Consider, for example, a non-local momentum structure in the center of mass frame of the type

$$(\mathbf{k}_3 + \mathbf{k}'_3) \cdot (\mathbf{k}_3 - \mathbf{k}'_3) = (\mathbf{q}' + \mathbf{q}) \cdot (\mathbf{q}' - \mathbf{q}). \quad (16)$$

Such terms can be treated by factorizing the momentum dependence like in Eq. (9), for example:

$$\mathbf{q} \cdot \mathbf{q}' = qq' \frac{4\pi}{3} \sum_{\mu_1, \mu_2 = -1}^1 Y_{1\mu_1}^*(\hat{\mathbf{q}}) Y_{1\mu_2}^*(\hat{\mathbf{q}}') \mathbf{e}_{\mu_1} \cdot \mathbf{e}_{\mu_2} \quad (17)$$

and then following exactly the steps like after Eq. (9). Obviously, the algorithm becomes less efficient for non-local interactions, but the current framework turns out to be still more efficient than the conventional approach for the relativistic corrections to chiral 3NF at N^3LO .

Generally, 3N interactions can be decomposed in terms of Faddeev components:

$$V_{123} = \sum_{i=1}^3 V_{123}^{(i)}, \quad (18)$$

whereas each of the three Faddeev components $V_{123}^{(i)}$ is symmetric in the particle labels $j, k \neq i \in \{1, 2, 3\}$ and the components are related via permutation transformations:

$$V_{123}^{(2)} = P_{123} V_{123}^{(1)} P_{123}^{-1}, \quad V_{123}^{(3)} = P_{132} V_{123}^{(1)} P_{132}^{-1}. \quad (19)$$

Here P_{123} (P_{132}) are the permutation operators that permute three particles cyclically (anti-cyclically) (see Ref. [40]). The decomposition (18) does not uniquely define the Faddeev components, and the specific values of matrix elements $V_{123}^{(i)}$ are generally convention-dependent. However, if evaluated between antisymmetrized wave functions, all choices and all Faddeev components give the same results. In contrast, the matrix elements of the completely antisymmetrized interaction,

$$V_{123}^{\text{as}} = (1 + P_{123} + P_{132}) V_{123}^{(i)} (1 + P_{123}^{-1} + P_{132}^{-1}), \quad (20)$$

are unique. Since the application of the permutation operators in Eq. (20) in a momentum partial wave basis is non-trivial and can induce numerical uncertainties (see Ref. [39]), we calculate and provide matrix elements of both $\langle pq\alpha|V_{123}^{(i)}|p'q'\alpha'\rangle$ and $\langle pq\alpha|V_{123}^{\text{as}}|p'q'\alpha'\rangle$. This offers the flexibility to transform the matrix elements of the Faddeev components to a harmonic oscillator basis and perform the antisymmetrization directly in this basis. The resulting matrix elements can then be used for calculations within e.g. the no-core shell model, the valence-shell model, the coupled cluster or the self-consistent Green's function framework. On the other hand, the antisymmetrized matrix elements $\langle pq\alpha|V_{123}^{\text{as}}|p'q'\alpha'\rangle$ can be directly used for studies of infinite nuclear matter or few-body scattering processes. Due to the large basis sizes shown in Table I, the uncertainties induced by the antisymmetrization are very small. We have checked that for three-nucleon systems the obtained binding energies based on the Faddeev components and the antisymmetrized interactions are identical within the sub-keV level.

For the application of the permutation operator P_{123} in the three-body plane-wave basis defined in Eq. (8) it is important to implement this operator in an efficient and numerically stable way. This is in particular important for calculations in large bases such as those shown in Table I. Several different expressions have been derived for the permutation operator (see, e.g., [40, 41]). All these expressions suffer from problems due to ratios of possibly very small numerators and denominators, which can lead to numerical instabilities for partial waves with large angular momenta. For our calculations, we use a novel improved implementation. Following the derivations of Ref. [40], it is straightforward to derive the following expression:

$$\begin{aligned}
\langle pq\alpha|P_{123}|p'q'\alpha'\rangle &= \sum_{\mathcal{L},\mathcal{S}} \sqrt{\widehat{j}\widehat{j}'\widehat{j}\widehat{j}'\widehat{S}} \\
&\times \begin{Bmatrix} L & S & J \\ l & 1/2 & j \\ \mathcal{L} & \mathcal{S} & \mathcal{J} \end{Bmatrix} \begin{Bmatrix} L' & S' & J' \\ l' & 1/2 & j' \\ \mathcal{L} & \mathcal{S} & \mathcal{J} \end{Bmatrix} \\
&\times (-1)^{S'} \sqrt{\widehat{S}\widehat{S}'} \begin{Bmatrix} 1/2 & 1/2 & S \\ 1/2 & S & S' \end{Bmatrix} \\
&\times (-1)^{T'} \sqrt{\widehat{T}\widehat{T}'} \begin{Bmatrix} 1/2 & 1/2 & T \\ 1/2 & \mathcal{T} & T' \end{Bmatrix} \\
&\times 8\pi^2 \int d\cos\theta_{\mathbf{p}\mathbf{q}} \frac{\delta(p' - |1/2\mathbf{p} + 3/4\mathbf{q}|)}{p'^2} \frac{\delta(q' - |\mathbf{p} - 1/2\mathbf{q}|)}{q'^2} \\
&\times \sum_{m_{\mathcal{L}}} \mathcal{Y}_{Ll}^{\mathcal{L}m_{\mathcal{L}}}(\widehat{\mathbf{p}\mathbf{q}}) \mathcal{Y}_{L'l'}^{\mathcal{L}m_{\mathcal{L}}}(-1/2\widehat{\mathbf{p}} - 3/4\widehat{\mathbf{q}}, \widehat{\mathbf{p}} - 1/2\widehat{\mathbf{q}}). \quad (21)
\end{aligned}$$

The key difference to other expressions is the fact that we directly perform the angular integrals as shown in Eq. (21) without decomposing the angular dependence of the spherical harmonic functions any further. This implementation turns out to be numerically more efficient

and, most importantly, is perfectly stable even for large values of angular momenta. The matrix elements of the operator P_{123} are also given by Eq. (21) (see Ref. [40]).

As a first application, we use the new framework to calculate the matrix elements of the chiral 3NF up to N³LO. The individual topologies are shown in Fig. 1. In addition to the pion decay coupling F_π and nucleon axial-vector coupling constant g_A , the chiral 3NFs up to N³LO depend on 7 LECs in total, namely $c_1, c_3, c_4, c_D, c_E, C_S$ and C_T [7–9, 42], for which we want to keep the flexibility of being able to change their values after performing the partial-wave decomposition. Specifically, the individual topologies are¹ (see also Fig. 1): (a) 2 π exchange [$c_1, c_3, c_4, 1$], (b) 1 π -contact [c_D], (c) pure contact [c_E], (d) 2 π -1 π exchange [1], (e) ring contributions [1], (f) 2 π -contact [C_T] and (g) relativistic corrections [$C_S, C_T, 1$]. Here, the couplings in square brackets denote those free LECs which appear in each of these topologies, whereas the constant '1' indicates contributions that do not contain any of the indicated 7 LECs. This leads in total to 12 individual contributions for each three-body partial wave as defined in Eq. (8).

For each of these contributions we first compute one of the Faddeev components $\langle pq\alpha|V_{123}^{(i)}|p'q'\alpha'\rangle$ for all partial wave channels and basis sizes shown in Table I. Subsequently, for the calculation of the antisymmetrized matrix elements $\langle pq\alpha|V_{123}^{\text{as}}|p'q'\alpha'\rangle$ we apply the permutation operator as defined in Eq. (21). The application of the permutation operator in the partial wave basis involves, in principle, a complete sum over intermediate partial wave quantum numbers (see, e.g., Ref. [39]). Thanks to the large basis sizes shown in Table I, we ensure that the antisymmetrization leads to well-converged results. Furthermore, it is straightforward to generate arbitrary other products of the permutation operator P_{123} and the Faddeev components in a computationally very efficient way. Such products appear, for example, in Faddeev equations for few-body scattering problems [41].

III. APPLICATION OF CHIRAL 3N FORCES AT N³LO TO NUCLEAR MATTER AND ³H

Figs. 2 and 3 illustrate the convergence of the partial wave expansion of the calculated chiral 3NFs. These figures show the 3NF contributions to the energy per particle of neutron matter (Fig. 2) and symmetric nuclear matter (Fig. 3) in Hartree-Fock approximation for the individual partial-wave channels and 3NF topologies. These results provide direct insight in the required number of partial-wave channels in mean-field calculations. Of course, the number of required partial-wave channels

¹ We correct a misprint in Eq. (4.14) of Ref. [9] and use the parameter values $\beta_8 = \frac{1}{4}$ and $\beta_9 = -\frac{1}{4}$, corresponding to the "minimal nonlocality" choice of the potential (see Ref. [15]).

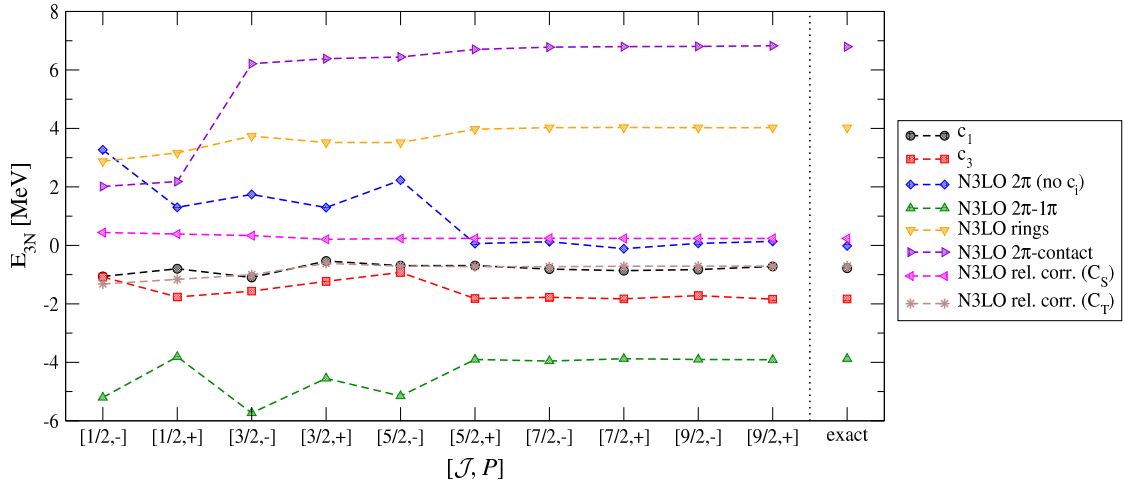


FIG. 2. (color online) Partial wave contributions to the energy per particle to neutron matter in the Hartree-Fock approximation at nuclear saturation density ($k_F^n = 1.7 \text{ fm}^{-1}$) for the individual 3NF topologies up to N^3LO . For the shown energies we use the coupling constants $C_S = C_T = 1$ and $c_i = 1 \text{ GeV}^{-1}$. All results show the accumulated energy contributions, including all contributions up to the given partial-wave channel. Here P denotes the three-body parity $P = (-1)^{L+l}$ and \mathcal{J} is the three-body total angular momentum, as defined in Eq. (8). In neutron matter only channels with $\mathcal{T} = 3/2$ contribute. The exact benchmark results are calculated following Refs. [17, 18].

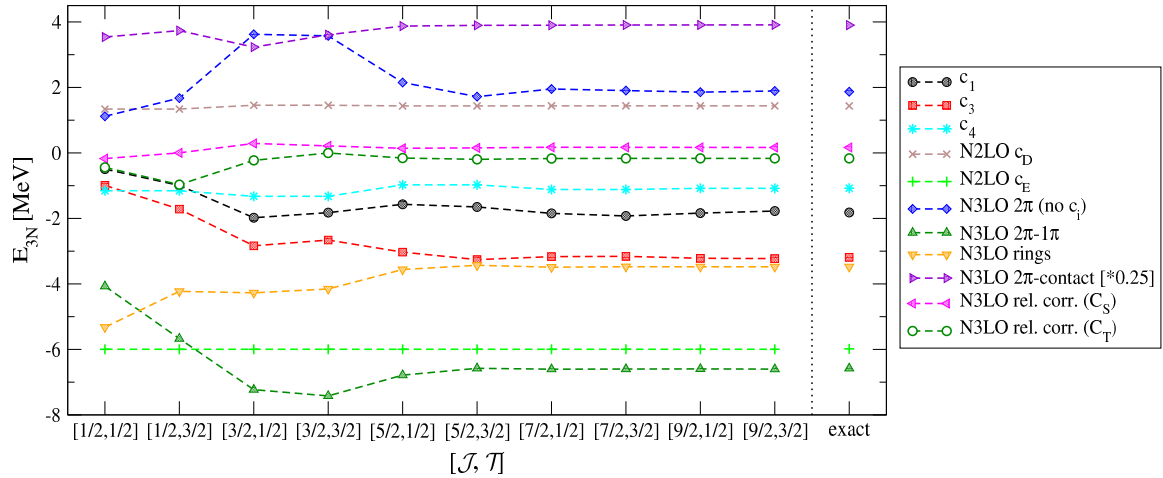


FIG. 3. (color online) Partial wave contributions to the energy per particle to symmetric nuclear matter in Hartree-Fock approximation at nuclear saturation density ($k_F^n = k_F^p = 1.35 \text{ fm}^{-1}$) for the individual 3NF topologies up to N^3LO . For the shown energies we use the coupling constants $C_S = C_T = 1$ and $c_i = 1 \text{ GeV}^{-1}$. The results for the 2π -contact topology are scaled by a factor of $1/4$ for presentation purposes. All results show accumulated energies, including all contributions up to the given partial-wave channel including both three-body parities. \mathcal{J} and \mathcal{T} are the three-body total angular momentum and isospin, as defined in Eq. (8). The exact benchmark results are calculated following Ref. [18].

has to be checked in more detail in realistic nuclear structure calculations, for which also many-body correlations are important. Moreover, these results also serve as a direct benchmark of the calculated matrix elements, since the energy contributions in the Hartree-Fock approximation have been already calculated independently based on the operator expressions directly, see Refs. [17, 18] for details.

Specifically, for the results shown in Fig. 2 we use $k_F = 1.7 \text{ fm}^{-1}$ for the neutron Fermi momentum, which corresponds to a neutron number density of $n \simeq 0.166 \text{ fm}^{-3}$.

Since the Fermi momentum serves as an ultraviolet cut-off, we do not need to regularize the interactions for these benchmark calculations. In neutron matter only matrix elements in the three-body isospin channel $\mathcal{T} = 3/2$ contribute, whereas the N^2LO topologies that include the low-energy coupling constants c_4 , c_D and c_E vanish exactly [43]. The detailed expressions for the Hartree-Fock energies for neutron matter in terms of the antisymmetrized matrix elements V_{123}^{as} are given in Ref. [44]. The results of Fig. 2 show that matrix elements up to the partial wave channel with $\mathcal{J} = 5/2$ and both three-body

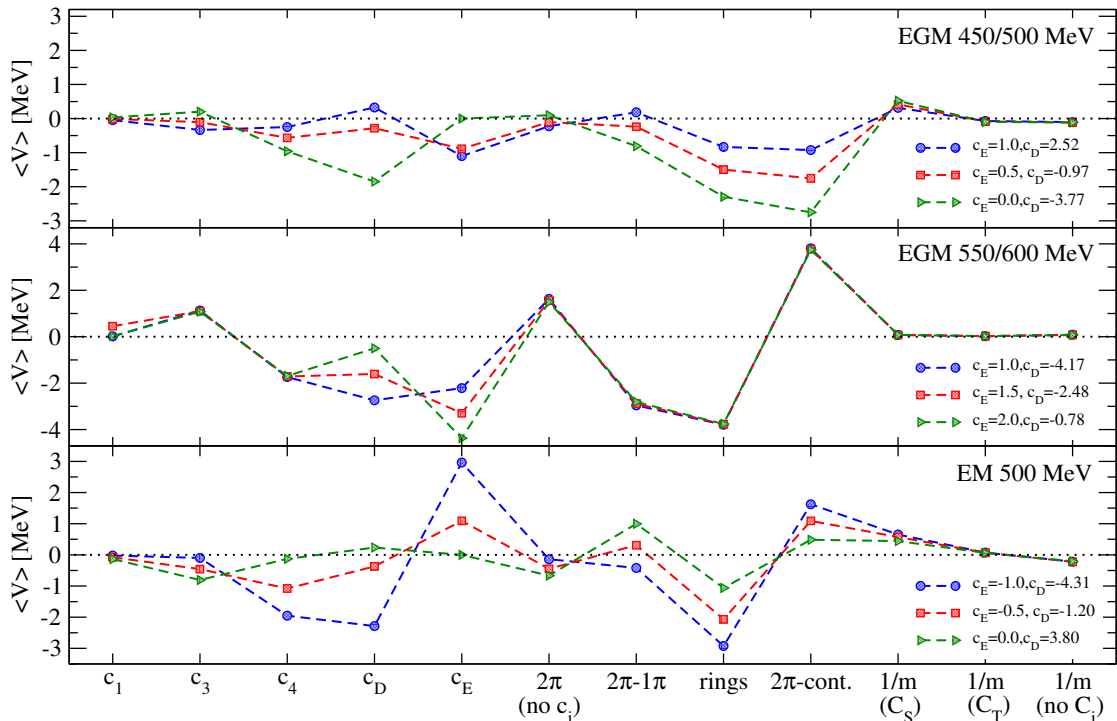


FIG. 4. (color online) Contributions of the individual topologies to the triton energy for three different NN interactions of Refs. [11, 22]. The LECs c_D and c_E are chosen to be of natural size and are fitted to the experimental triton binding energy. The topologies c_1 , c_3 and c_4 contain contributions from N^2 LO and N^3 LO, c_D and c_E are pure N^2 LO contributions and 2π (no c_i), $2\pi-1\pi$, rings, 2π -cont and $1/m$ corrections are N^3 LO contributions. See main text for details.

parities $P = (-1)^{L+l}$ can provide significant contributions to the energy, whereas higher partial waves give only small corrections. Overall, we find that the results including all contributions up to $\mathcal{J} = 9/2$ are very well converged and show excellent agreement with the exact results (see also [45]).

For symmetric nuclear matter we find a very similar convergence pattern. In contrast to neutron matter here all 3NF topologies shown in Fig. 1 and also both three-body isospin channels, $\mathcal{T} = 1/2$ and $\mathcal{T} = 3/2$, contribute to the energy. For the results shown in Fig. 3 we fix the neutron and proton Fermi momenta to $k_F^n = k_F^p = 1.35 \text{ fm}^{-1}$, which again corresponds to a total number density of $n \simeq 0.166 \text{ fm}^{-3}$. We show the contributions to the energy for the individual partial-wave channels, whereas here each $[\mathcal{J}, \mathcal{T}]$ channel includes contributions from both three-body parity channels $P = \pm 1$. Again, we observe excellent partial wave convergence and essentially perfect agreement with the exact Hartree-Fock results.

Next, in Fig. 4 we illustrate the contributions of the individual topologies to the binding energy of ${}^3\text{H}$. In order to probe scheme dependence of our results, the present calculations use three different NN interactions: the N^3 LO potentials of Ref. [12] with the cutoff combinations $\Lambda/\tilde{\Lambda} = 450/500 \text{ MeV}$ and $550/600 \text{ MeV}$ (EGM) and the N^3 LO potential of Ref. [11] (EM). For our calculations we fix the values of the LECs c_1, c_3, c_4, C_S and C_T

consistently to their values of the NN interactions. Notice further that the N^3 LO corrections to the two-pion exchange topology involve contributions which account for finite shifts in the LECs c_i in the N^2 LO 3NF expressions [8]. All these effects are properly taken into account. The couplings c_D and c_E are fixed to the experimental binding energy of ${}^3\text{H}$ and by requiring the values of those LECs to be of natural size. For each of the NN potentials we used three sets of values, their specific values for the different interactions are given in the legend of Fig. 4. The matrix elements of the 3NF are regularized by applying a non-local regulator of the form $f_R(p, q) = \exp[-((p^2 + 3/4q^2)/\Lambda_{3N}^2)^3]$ as in Ref. [46], whereas the value of the cutoff Λ_{3N} is chosen to be consistent with the cutoff value Λ of the corresponding NN interaction. Note that all results of this figure are based on the consistent wave functions for each of these fits, which obviously complicates a detailed quantitative comparison of results based on different fits or NN interactions. However, we do not expect that this affects the main qualitative features of the results, which can be summarized as follows: first, the size of the contributions of the individual topologies depends sensitively on the employed NN interaction as well as on the values of the LECs c_D and c_E . Second, the contributions of topologies at N^3 LO are not suppressed compared to those at N^2 LO for the presently employed 3N interactions. Similar findings have been found before for ${}^3\text{H}$ using a restricted

number of partial waves [47] and for the mean-field contributions of the $N^3\text{LO}$ 3NFs to neutron matter and symmetric matter [17, 18]. Third, the perturbativeness of the 3NFs also depends sensitively on the employed NN interaction. While, e.g., for the interaction EGM 550/600 the wave function is not strongly affected by variations of the short-range couplings, for the other two NN interactions the contributions from the long-range 3N topologies also change when the LECs c_D and c_E are varied.

When interpreting these results, it is important to keep in mind that neither the individual nor the total contribution of the 3NFs to the binding energies of nuclei are experimentally observable. The considered contributions of individual topologies represent, strictly speaking, bare quantities while all estimations based on power counting refer to renormalized ones, see also Ref. [47]. Moreover, the employed nonlocal regulators do not actually cut off all short-range pieces of the 3NFs, so even the long-range 3NF topologies do contain short-range contributions after regularization (see Ref. [15] for a related discussion).

Clearly, expectation values of such short-range admixtures are strongly scheme dependent. Recently, a novel type of chiral NN interactions has been developed [15, 48, 49]. For these new interactions, the long-range topologies are regularized by local regulators that act only on the relative particle distance in coordinate space and allow for a cleaner separation of long- and short-distance physics. Indeed, in Ref. [50] it was shown explicitly that 2π -exchange contributions dominate at long- and intermediate distances when local regulators are employed for NN interactions.

IV. SUMMARY AND OUTLOOK

In summary, the new framework presented in this work makes it possible to include the chiral 3NF at $N^3\text{LO}$ and beyond in ab initio few- and many-body calculations. For non-local regulators, the calculated matrix elements can be immediately used within various many-body frameworks for novel studies including all NN and 3N contributions consistently beyond $N^2\text{LO}$. The application of the regularization scheme employed in Ref. [10, 15] for the NN forces to 3NF will require a generalization of the present framework. In contrast to the considered non-local regulators, which only depend on the magnitude of the Jacobi momenta and act just as multiplicative factors in momentum space, local regulators do mix different partial waves. The application of these regulators in momentum space can, e.g., be implemented using their partial wave decomposed form and performing numerical evaluation of the corresponding folding integrals. Work along this line is in progress.

We also emphasize that a careful investigation of systematic uncertainties in few- and many-nucleon calculations represents an important goal in nuclear physics, see also discussions in Refs. [15, 51]. The availability of matrix elements of NN and 3N interactions at different

orders in the chiral expansion and within different regularization schemes will provide an important contribution towards a better understanding of the systematic uncertainties and ultimately allow for precision tests of chiral dynamics in nuclear systems. Last but not least, we emphasize that the presented framework can be straightforwardly applied to 3NF at order $N^4\text{LO}$ [52, 53] and to EFT interactions with explicit Δ -degrees of freedom [54].

ACKNOWLEDGMENTS

We thank V. Durant, R. J. Furnstahl, A. Schwenk for helpful comments, T. Krüger and I. Tews for providing the exact benchmark Hartree-Fock results for neutron matter and nuclear matter, K. Topolnicki and H. Witała for their contribution to the partial-wave framework we used for testing the calculated matrix elements, and C. Drischler for performing additional test calculations. The present work was supported by the ERC Grants No. 307986 STRONGINT and 259218 NUCLE-AREFT, by the Helmholtz Alliance HA216/EMMI, by the European Community-Research Infrastructure Integrating Activity ‘‘Study of Strongly Interacting Matter’’ (acronym HadronPhysics3, Grant Agreement n. 283286) under the Seventh Framework Programme of EU, and by awards of computational resources from the Ohio Supercomputer Center and from the Jülich Supercomputing Center. The work of the Cracow group was supported by the Polish National Science Center under Grant No. DEC-2013/10/M/ST2/00420.

Appendix A: Appendix: Angular integrations in partial wave decomposition

In this Appendix we describe the integral transformations which allow for a decoupling of the three non-trivial integrations over spherical harmonics in the partial wave decomposition of the 3NF from the other five which can be performed analytically. Let us start with the Eq. (3) and add a radial integration over \tilde{p}' and \tilde{q}' in order to have a translationally invariant measure. We can achieve this by introducing additional integrations with delta-functions via

$$\begin{aligned}
 F_{LL'L'}^{m_L m_l m_{L'} m_{l'}}(p, q, p', q') &= \frac{1}{p'^2 q'^2} \int d^3\tilde{q}' d^3\tilde{p}' d\hat{\mathbf{q}} d\hat{\mathbf{p}} \\
 &\times \delta(p' - \tilde{p}') \delta(q' - \tilde{q}') Y_{L'm_{L'}}^*(\hat{\mathbf{p}}') Y_{l'm_{l'}}^*(\hat{\mathbf{q}}') Y_{Lm_L}(\hat{\mathbf{p}}) Y_{lm_l}(\hat{\mathbf{q}}) \\
 &\times V_{123}^{\text{loc}}(\tilde{\mathbf{p}}' - \mathbf{p}, \tilde{\mathbf{q}}' - \mathbf{q}). \tag{A1}
 \end{aligned}$$

Now we can make a substitution

$$\tilde{\mathbf{p}}' \rightarrow \tilde{\mathbf{p}}' + \mathbf{p} \quad \text{and} \quad \tilde{\mathbf{q}}' \rightarrow \tilde{\mathbf{q}}' + \mathbf{q}, \tag{A2}$$

which leads to

$$F_{L'L''}^{m_L m_{L'} m_{L''}}(p, q, p', q') = \frac{1}{p'^2 q'^2} \int d^3 \tilde{q}' d^3 \tilde{p}' d\hat{q} d\hat{p} \\ \times \delta(p' - |\tilde{\mathbf{p}}' + \mathbf{p}|) \delta(q' - |\tilde{\mathbf{q}}' + \mathbf{q}|) V_{123}^{\text{loc}}(\tilde{q}', \tilde{p}', \cos \theta'_{\tilde{\mathbf{p}}' \tilde{\mathbf{q}}'}) \\ \times Y_{L'm_{L'}}^*(\widehat{\tilde{\mathbf{p}}' + \mathbf{p}}) Y_{L''m_{L''}}^*(\widehat{\tilde{\mathbf{q}}' + \mathbf{q}}) Y_{Lm_L}(\hat{\mathbf{p}}) Y_{lm_l}(\hat{\mathbf{q}}). \quad (\text{A3})$$

In this form it is manifest that the integrals factorize and we need to calculate

$$\frac{1}{p'^2 q'^2} \int d\hat{q} d\hat{p} d\hat{p}' \int_0^{2\pi} d\phi_{\tilde{q}'} \delta(p' - |\tilde{\mathbf{p}}' + \mathbf{p}|) \delta(q' - |\tilde{\mathbf{q}}' + \mathbf{q}|) \\ \times Y_{L'm_{L'}}^*(\widehat{\tilde{\mathbf{p}}' + \mathbf{p}}) Y_{L''m_{L''}}^*(\widehat{\tilde{\mathbf{q}}' + \mathbf{q}}) Y_{Lm_L}(\hat{\mathbf{p}}) Y_{lm_l}(\hat{\mathbf{q}}), \quad (\text{A4})$$

where $\phi_{\tilde{q}'}$ is an azimuthal angle of $\hat{\mathbf{q}}'$. This integral does not involve the 3NF and can be calculated analytically. The full result is given by Eq. (6).

-
- [1] N. Kalantar-Nayestanaki, E. Epelbaum, J. G. Messchendorp and A. Nogga, Rept. Prog. Phys. **75**, 016301 (2012).
- [2] H.-W. Hammer, A. Nogga, and A. Schwenk, Rev. Mod. Phys. **85**, 197 (2013).
- [3] S. Weinberg, Phys. Lett. B **251**, 288 (1990).
- [4] U. van Kolck, Phys. Rev. C **49**, 2932 (1994).
- [5] E. Epelbaum, H.-W. Hammer and U.-G. Meißner, Rev. Mod. Phys. **81**, 1773 (2009).
- [6] R. Machleidt and D. R. Entem, Phys. Rept. **503**, 1 (2011).
- [7] S. Ishikawa and M. R. Robilotta, Phys. Rev. C **76**, 014006 (2007).
- [8] V. Bernard, E. Epelbaum, H. Krebs and U.-G. Meißner, Phys. Rev. C **77**, 064004 (2008).
- [9] V. Bernard, E. Epelbaum, H. Krebs and U.-G. Meißner, Phys. Rev. C **84**, 054001 (2011).
- [10] E. Epelbaum, H. Krebs and U.-G. Meißner, arXiv:1412.4623 [nucl-th]
- [11] D. R. Entem and R. Machleidt, Phys. Rev. C **68**, 041001(R) (2003).
- [12] E. Epelbaum, W. Glöckle and U.-G. Meißner, Nucl. Phys. A **747**, 362 (2005).
- [13] A. Ekström *et al.*, Phys. Rev. Lett. **110**, 192502 (2013).
- [14] A. Gezerlis, I. Tews, E. Epelbaum, S. Gandolfi, K. Hebeler, A. Nogga and A. Schwenk, Phys. Rev. Lett. **111**, 032501 (2013).
- [15] E. Epelbaum, H. Krebs and U.-G. Meißner, arXiv:1412.0142 [nucl-th].
- [16] J. Golak *et al.*, Eur. Phys. J. A **50**, 177 (2014).
- [17] I. Tews, T. Krüger, K. Hebeler, and A. Schwenk, Phys. Rev. Lett. **110**, 032504 (2013).
- [18] T. Krüger, I. Tews, K. Hebeler, and A. Schwenk, Phys. Rev. C **88**, 025802 (2013).
- [19] Low Energy Nuclear Physics International Collaboration, <http://www.lenpic.org>.
- [20] S. Binder, J. Langhammer, A. Calci, and R. Roth, Phys. Lett. **B** 736, 119 (2014).
- [21] S. C. Pieper, V. R. Pandharipande, R. B. Wiringa and J. Carlson, Phys. Rev. C **64**, 014001 (2001).
- [22] E. Epelbaum, Prog. Part. Nucl. Phys. **57**, 654 (2006).
- [23] J. W. Holt, N. Kaiser and W. Weise, Prog. Part. Nucl. Phys. **73**, 35 (2013).
- [24] E. Epelbaum, H. Krebs, D. Lee and U.-G. Meißner, Phys. Rev. Lett. **104**, 142501 (2010).
- [25] E. Epelbaum, H. Krebs, D. Lee and U.-G. Meißner, Phys. Rev. Lett. **106**, 192501 (2011).
- [26] E. Epelbaum, H. Krebs, T. A. Lahde, D. Lee and U.-G. Meißner, Phys. Rev. Lett. **109**, 252501 (2012).
- [27] R. Roth, J. Langhammer, A. Calci, S. Binder and P. Navratil, Phys. Rev. Lett. **107**, 072501 (2011).
- [28] B. R. Barrett, P. Navratil and J. P. Vary, Prog. Part. Nucl. Phys. **69**, 131 (2013).
- [29] F. Wienholtz *et al.*, Nature **498**, 346 (2013).
- [30] T. Otsuka, T. Suzuki, J. D. Holt, A. Schwenk and Y. Akaishi, Phys. Rev. Lett. **105**, 032501 (2010).
- [31] J. D. Holt, T. Otsuka, A. Schwenk and T. Suzuki, J. Phys. G **39**, 085111 (2012).
- [32] H. Hergert, S. Binder, A. Calci, J. Langhammer and R. Roth, Phys. Rev. Lett. **110**, 242501 (2013).
- [33] V. Somà, A. Cipollone, C. Barbieri, P. Navratil and T. Duguet, Phys. Rev. C **89**, 061301 (2014).
- [34] G. Hagen, M. Hjorth-Jensen, G. R. Jansen, R. Machleidt and T. Papenbrock, Phys. Rev. Lett. **108**, 242501 (2012).
- [35] S. K. Bogner, A. Schwenk, R. J. Furnstahl and A. Nogga, Nucl. Phys. A **763**, 59 (2005).
- [36] K. Hebeler, S. K. Bogner, R. J. Furnstahl, A. Nogga and A. Schwenk, Phys. Rev. C **83**, 031301(R) (2011).
- [37] P. Navratil, Few Body Syst. **41**, 117 (2007).
- [38] J. Golak *et al.*, Eur. Phys. J. A **43**, 241 (2010).
- [39] R. Skibiński *et al.*, Eur. Phys. J **47**, 48 (2011).
- [40] W. Glöckle, *The Quantum Mechanical Few-Body Problem* (Springer-Verlag, Berlin, 1983).
- [41] W. Glöckle, H. Witala, D. Huber, H. Kamada and J. Golak W. Glöckle, Phys. Rept. **274**, 107 (1996).
- [42] E. Epelbaum, A. Nogga, W. Gloeckle, H. Kamada, U.-G. Meissner and H. Witala, Phys. Rev. C **66**, 064001 (2002).
- [43] K. Hebeler and A. Schwenk, Phys. Rev. C **82**, 014314 (2010).
- [44] K. Hebeler and R. J. Furnstahl, Phys. Rev. C **87**, 031302(R) (2013).
- [45] C. Drischler, Master Thesis, TU Darmstadt (2014).
- [46] E. Epelbaum *et al.*, Phys. Rev. C **66**, 064001 (2002).
- [47] R. Skibiński *et al.*, Phys. Rev. C **84**, 054005 (2011).
- [48] A. Gezerlis, I. Tews, E. Epelbaum, S. Gandolfi, K. Hebeler, A. Nogga and A. Schwenk, Phys. Rev. Lett. **111**, 032501 (2013).
- [49] A. Gezerlis, I. Tews, E. Epelbaum, M. Freunek, S. Gandolfi, K. Hebeler, A. Nogga and A. Schwenk, Phys. Rev. C **90**, 054323 (2014).
- [50] E. Epelbaum, A. M. Gasparyan, H. Krebs and C. Schat, arXiv:1411.3612 [nucl-th].
- [51] R. J. Furnstahl, D. R. Phillips, and S. Wesolowski, arXiv:1407.0657 [nucl-th].
- [52] H. Krebs, A. Gasparyan, and E. Epelbaum, Phys. Rev. C **85**, 054006 (2012).

- [53] H. Krebs, A. Gasparyan, and E. Epelbaum, Phys. Rev. C **87**, 054007 (2013).
- [54] E. Epelbaum, H. Krebs and U.-G. Meißner, Nucl. Phys. A **806**, 65 (2008).